Original article

Institution of MECHANICAL ENGINEERS
Journal of MATERIALS: DESIGN AND APPLICATIONS

Proc IMechE Part L:
J Materials: Design and Applications
2020, Vol. 234(1) 167–174

DOI: 10.1177/1464420719880935
journals.sagepub.com/home/pil
SAGE

Characterization and application of a selective coating for solar collectors from of the cashew nut shell liquid

Diego Caitano Pinho[1], Francisco Nivaldo Aguiar Freire[1], Felipe Alves Albuquerque Araújo[1], Kaio Hemerson Dutra[1], Edwalder Silva Teixeira[1], Maria Eugênia Vieira da Silva[2] and Paulo Alexandre Costa Rocha[2]

Abstract

Solar energy is the most promising energy source, due to its great availability and applicability in thermal energy applications. However, researchers still experience technological and economical challenge, since many systems that use this energy still have low efficiency and high cost. In this way, the development of new materials and technologies to increase the efficiency of solar thermal collectors is both a challenge and a necessity. In this context, the objective of this work is to obtain and analyze selective surfaces for solar thermal collectors, using cashew nut shell liquid. The cashew nut shell liquid can be classified as technical or natural, depending on the mode of extraction of cashew liquid. An experimental bench was built to simulate a flat plate solar collector under real operating conditions. For comparative purposes, the tests were performed between the cashew nut shell liquid and the commercial surface (MRTiNOX). In order to verify the structure morphology and the chemical composition of the surface, analyzes were performed by scanning electron microscopy. In order to identify the presence of components after the sintering process, the infrared analysis technique was used. To analyze the surface absorbance, the ultraviolet–visible spectroscopy absorbance technique was used. With the tests in real conditions, it was possible to perform the temperature measurements, and later, with the energy balance, the absorptivity, emissivity, and efficiency were calculated. The technical cashew nut shell liquid presented efficiency of 42.86%, while the MRTiNOX, 41.8%. In contrast, natural cashew nut shell liquid obtained efficiency of 31.28%. Thus, the use of technical cashew nut shell liquid, a low-cost regional product, was presented as a viable and satisfactory solution for cost reduction in solar thermal collectors.

Keywords

Solar energy, collectors, selective surface, cashew nut shell liquid, efficiency

Date received: 30 May 2019; accepted: 15 September 2019

Introduction

The depletion of fossil fuel reserves and climate change caused by atmospheric pollution has led the human being to seek alternatives that are less harmful to the environment.[1] Concern and awareness of the population together with the growing world demand for energy, opens space for the study of renewable energies,[2] among them, the best use of solar energy, considered as the most abundant source of energy renewable energy.

Solar energy is abundant, renewable, and clean. Theoretically, solar energy has the potential to adequately meet the energy demands of the world if technologies for your harvested and supply are available.[3] Approximately four million solar energy exajoule reaches the earth annually, and only 5×10^4, of what is expected is harvested.[4]

The Sun works as an immense fusion reactor, irradiating daily a high-energy potential, incomparable to any other energy system.[5] Solar radiation can be absorbed and collected through a device called the solar collector, which directly converts the solar

[1]Universidade Federal do Ceará, Laboratório em Filmes Finos em Energia Renováveis, Fortaleza, Brasil
[2]Universidade Federal do Ceará, Laboratório em Energia solar e Gás Natural, Fortaleza, Brasil

Corresponding author:
Diego Caitano Pinho, Universidade Federal do Ceará, Av. da Universidade, 2853 Fortaleza, 60020-181 Brazil.
Email: diegopynho@gmail.com

radiation of solar electromagnetic waves in thermal energy and transfers that energy with flow fluid—such as air, water, or oil—contained within the collectors.[6]

In general, solar collectors capture solar radiation through the absorptive spectral region and transform it into thermal energy. This region can be obtained by a black surface or a selective surface, the latter being more efficient. However, in order for the energy conversion efficiency to increase—and consequently raise the system stagnation temperature—the absorber plate must have a coating with selective characteristics, absorbing the maximum of radiation in the ultraviolet, visible, and near-infrared spectra and having a minimum reflectance in the infrared region.

The objective of this work is to synthesize, analyze, and test selective surfaces for application in flat plate solar collectors using cashew nut shell liquid (CNSL). The purpose is to obtain a surface similar or superior to the selective surfaces already on the market.

Materials and methods

CNSL

Cashew agribusiness is very intense in Brazil, especially in the state of Ceará, which concentrates 8 of the 12 companies in the country and holds 70% of the installed capacity in the Northeast region. These Brazilian companies together process about 360,000 tons/year of cashew nuts that generate about 45,000 tons of CNSL/year.

CNSL makes up approximately one-third of the total cashew nut weight,[7] obtained from *Anacardium occidentale*, popularly known as cashew tree. Despite being a byproduct of agribusiness, CNSL is a source of natural origin rich in non-isoprenoid phenolic lipids.[8] CNSL—brown oil extracted from the processing of cashew nuts—composes 18% of the 27% of the total weight of the achene and has low added value.[9]

The CNSL can be classified as technical or natural, depending on the mode of extraction of cashew liquid. The technical CNSL is obtained through the extraction process involving the heating of the almonds at a temperature of 180–200 °C. When the anacardic acid is subjected to high temperatures, it undergoes a decarboxylation reaction and is converted to cardanol, producing the technical CNSL.[10] The technical CNSL contains mainly cardanol[11] (60–65%), cardol (15–20%), polymeric material (10%), and traces of methylcardol. The natural CNSL, in turn, is extracted by means of solvents and presses and it constituted anacardic acid (60–65%), cardol (15–20%), cardanol (10%), and traces of metilcardol.

Extraction of natural CNSL

To extract the CNSL natural used in this study, the cashew nuts were first bisected and then the almonds were removed. The shells (150 g) were immersed in a becker of 2 L containing 500 mL of hexane and heated at 75 °C for 2 h. After filtration, the extract was concentrated in a rotary evaporator to give a final natural CNSL mass of 70 mL.

Surfaces preparation

In the present work, the natural CNSL and the technical CNSL were used separately. CNSL is a viscous material, it is necessary to add the B_2O_3/Bi_2O_3 flux (to 1:1 mixture of boron–bismuth in a ratio of 1:1) to improve the adhesion of the mixture to the copper substrate. The sulfuric acid (H_2SO_4) was also added as a catalyst for better homogeneity of the surface on the copper substrate. The composition of each selective surface produced is shown in Table 1.

After obtaining the compounds, the deposition was made on a copper substrate (5 cm × 3 cm plate, about 0.3-mm thick) by the process known as screen printing, in which a spatula is used to perform the dispersing the compound on the substrate in a single direction. The surfaces were thermally treated (sintering) in a resistive kiln—following the configuration shown in Figure 1—at a heating rate of 0.5 °C/min, so that the H_2SO_4 evaporated and thus the sintering process was completed. The surface cooling occurred inside the kiln.

Test brench

To perform the field tests, an experimental bench was constructed with a 2.5-cm thick muiracatiara wooden box, with an MRVivix float glass cover, colorless, tempered, 1 m × 12.6 cm and 4-mm thick. The bench was divided into nine equal compartments,

Table 1. Composition of selective surface obtained.

Components	Surface 1	Surface 2
Technical CNSL (%)	93	–
Natural CNSL (%)	–	93
Flux (%)	3	3
H_2SO_4 (%)	4	4
Total mass (g)	1	1

CNSL: cashew nut shell liquid.

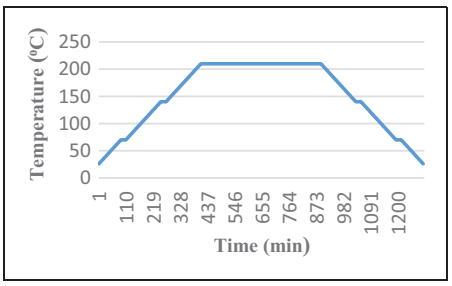

Figure 1. Sintering parameters.

Figure 2. Test bench.

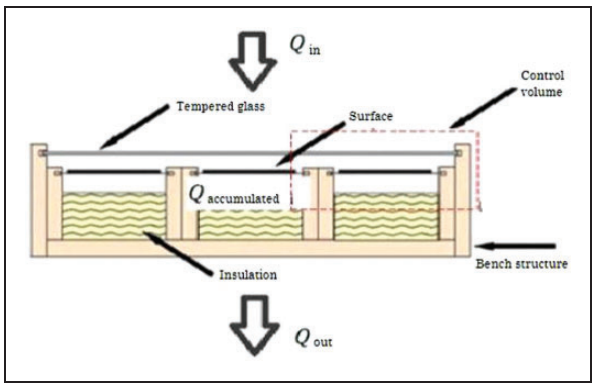

Figure 3. Representation test bench.

being covered at the bottom by rectangular pieces of glass wool, 11.5 cm × 8.5 cm and a thickness of 5 cm. The copper plates with the deposited selective surfaces were placed in each of these compartments above the glass wool insulation for testing in real conditions. In Figure 2, it shows the test bench.

The bench was composed of "k" type thermocouples,—for measuring the temperatures of the selective surfaces of the environment, glass and insulation—of an MREppley Horizontal Piranometer—for the measurement of solar radiation—and an Omega datalogger—to record and store the temperature data obtained during the tests.

Energy balance in the test bench

The energy balance in the test bench is necessary to compare the performance of the selective surfaces. Figure 3 shows the energy balance representation in the experimental apparatus.

The input energy (Q_{in}), equation (1), is related to the solar radiation transmitted through the glass (R_{sol}), with the transmissivity of the glass (τ_v), with absorptivity of the selective surface (α_s) and with the area of the plate (A_P). The output energy (Q_{out}) is related to the thermal losses through the collector by convection, conduction and thermal radiation.

$$Q_{in} = R_{sol}\tau_v\alpha_s A_P \tag{1}$$

In this system there is no loss through forced convection by the action of the wind due to the protection of the glass. Therefore, there will be only natural convection between the surface and the glass cover. The loss by natural convection is given by equation (2).

$$Q_{conv} = hA_P(T_P - T_{cg}) \tag{2}$$

where h is the heat transfer coefficient by convection, T_P is the plate temperature, and T_{cg} is the temperature of the glass cover.

The loss of energy by conduction occurs through the walls of wood of the test bench and by the thermal insulation. Equation (3) represents the energy losses by conduction.

$$Q_{cond} = (K/L)A_P(T_P - T_b) \tag{3}$$

where K is the thermal conductivity, L is the thickness of the insulation, and T_b is the temperature near to the outer wall of the structure. The radiation loss is given by equation (4).

$$Q_{rad} = \varepsilon A_P\sigma(T_P^4 - T_b^4) \tag{4}$$

where ε is the emissivity of the selective surface and σ is the Stefan–Boltzman constant ($\sigma = 5.6710^{18}\,\mathrm{W/m^2k^4}$).

The energy lost by reflection corresponds to the solar radiation reflected by the surface of the copper plates. The loss of energy by reflection is given by equation (5).

$$Q_{ref} = (1 - \alpha_s)R_{sol}A_P \tag{5}$$

The energy balance for the control volume shown in Figure 3 is given by equation (6).

$$Q_{accumulated} = Q_{in} - Q_{out} + Q_{transformed} \tag{6}$$

where the transformed heat rate ($Q_{transformed}$) is zero because there is not generation of energy.

So that the collector was not associated with a system of fluid during the time of exposure to the Sun, therefore, operating in permanent regime, the accumulated heat rate is zero. Then, substituting equations (1) to (5) into equation (6) and adopting the proposed considerations, the energy balance equation can be written as represented in equation (7).

$$R_{sol}\tau_v\alpha_s A_P = hA_P(T_P - T_{cg})\varepsilon A_P\sigma(T_P^4 - T_b^4) \times (K/L)A_P(T_P - T_b)(1 - \alpha_s)R_{sol}A_P \tag{7}$$

From equation (7) it is possible to calculate the absorptivity and emissivity properties of the selective surface based on the data obtained in the field tests. For this, it is necessary use equation (8), which corresponds the useful energy (Q_{useful}) supplied by a solar collector to the working fluid.[12]

$$Q_{useful} = A_P[R_{sol}\tau_v\alpha_s - U_l(T_P - T_a)] \quad (8)$$

where T_a is the ambient temperature.

As the operating conditions of all selective surfaces were the same, then the overall coefficient of heat loss (U_l) is the same for all surfaces. So, since there is no use of thermal fluid, $Q_{useful} = 0$. Therefore, equation (8) can be written as represented in equation (9).

$$U_l = R_{sol}\tau_v\alpha_s/(T_P - T_a) \quad (9)$$

Performed test

1. Absorbance graphs, in the range of 190–900 nm, obtained by the analysis of the selective surfaces deposited in glass, realized in a Cary Series ultraviolet–visible spectroscopy (UV–Vis) Spectrophotometer;
2. Performance tests of the selective surfaces in the test bench in real environmental conditions, with measurements of temperature, absorbance, and emittance;
3. Verification of the morphological structure and chemical composition resulting from the synthesization of the material by means of Energy Dispersive X-ray (EDX) micro scanning electron microscopy (SEM);
4. Infrared analysis, with KBr inserts, in the Shimadzu apparatus, IRTracer-100 model, in the range of 400–4000 cm^{-1}, in order to determine if any composites were formed after the surfaces preparation in the resistive kiln.

Results and discussions

Characterization by UV–Vis

The absorbance is one of the most important properties to analyze on a selective surface. The Shimadzu's spectrometer UV-2600 is used to measured the absorbance. The Figure 4 shows the graph plotted from the results obtained for the technical CNSL and the natural CNSL.

It is observed that in both surfaces, the absorbance in the visible light range (400–750 nm) has a maximum value, which is a positive characteristic for a better capture of solar energy. It is also noticed that the technical CNSL shows higher values in the visible light range compared to the natural CNSL.

Field tests

In the month of August 2018 were performed field tests on days 08, 09, 22, and 23. These tests were performed to analyze the behavior of the selective surfaces exposed to the Sun, with measurements of temperature, absorbance, and emittance.

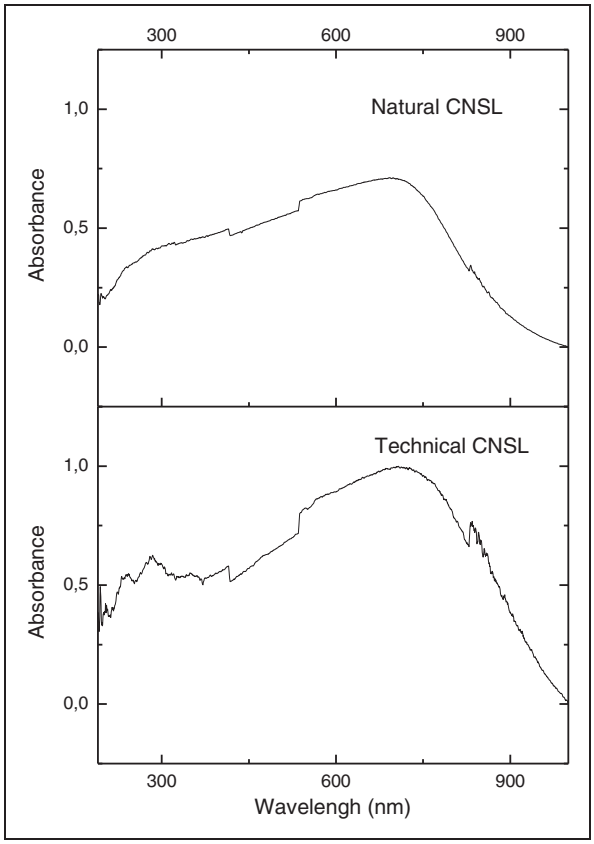

Figure 4. Absorbance graphs of selective surfaces produced.

The tested surfaces were: CNSL technical, CNSL natural, and TiNOX. The temperatures of the glass cover, the insulation and the environment were also measured. In these days of testing, the sky was clear with few clouds. On August 23 presented higher average radiation value 843 between 10h and 14:40h, the range in which the test bench was in operation; and 923 between 11h and 1h. Figure 5 shows the measurements of temperature and global radiation.

When the system reached steady state, measured from 11 h to 13 h, the temperature of the three surfaces was saved every 2 min: technical CNSL, natural CNSL, and MRTiNOX. Glass cover temperatures, insulation, and the environment were also measured. The temperature averages are given in Table 2.

To calculate the absorptivity, emissivity, and efficiency from the energy balance, it was necessary obtain data of the commercial surface manufacturer (MRTiNOX) and the glass used in the test bench. The manufacturer's data are presented in Table 3.

The insulation thickness (L) is 5 cm, thermal conductivity (K) of 0.04 W/mK. So, to calculate the overall loss coefficient (U_l), equation (9), was used the manufacture's data together with the average radiation of 923 W/m^2 in the interval of 11 h to 13 h. To calculate the heat transfer coefficient (h), we

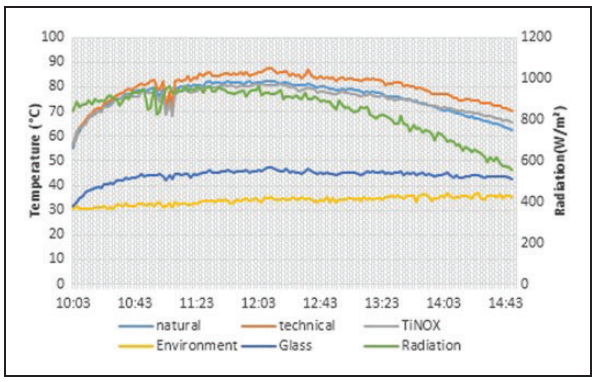

Figure 5. Comparison between average temperatures on selective surfaces.

Table 2. Average temperatures for steady-state operation.

Measured elements	Average temperature (°C)
Technical CNSL	89.1
Nature CNSL	86.4
MRTiNOX	88.9
Glass Cover	65.7
Insulation	33.7
Environment	33.7

CNSL: cashew nut shell liquid.

Table 3. Manufacturer's data.[13]

Materials	Absorbance (α_s)	emissivity (ε)	Transmissivity (τ_v)
Glass	–	–	0.87
MRTiNOX	0.95	0.04	–

Table 4. Results obtained for the coefficients.

Coefficient	Results obtained
Overall loss coefficient (U_l)	16.8
Heat transfer coefficient (h)	29.2 W/m^{2}K

apply equation (7) to the commercial surface, knowing that the area of the plate used was $A_P = 0.0015\,\text{m}^2$. Results obtained for the coefficients are presented in Table 4.

The result for heat transfer coefficient (h) is considered plausible, because in natural convection applications, the heat coefficient (h) can vary in a range from 5 to 30 W/m^{2}K.[14]

As the overall coefficient of heat loss is $U_l = 16.8$, and is the same for all selective surfaces, the absorbance values of the selective surfaces are obtained using

Table 5. Absorptivity and emissivity of selective surfaces.

Surface	Absorptivity	Emissivity	Efficiency
Technical CNSL	0.95	0.0222	42.86
Nature CNSL	0.90	0.0290	31.28
MRTiNOX	0.95	0.0226	41.85

CNSL: cashew nut shell liquid.

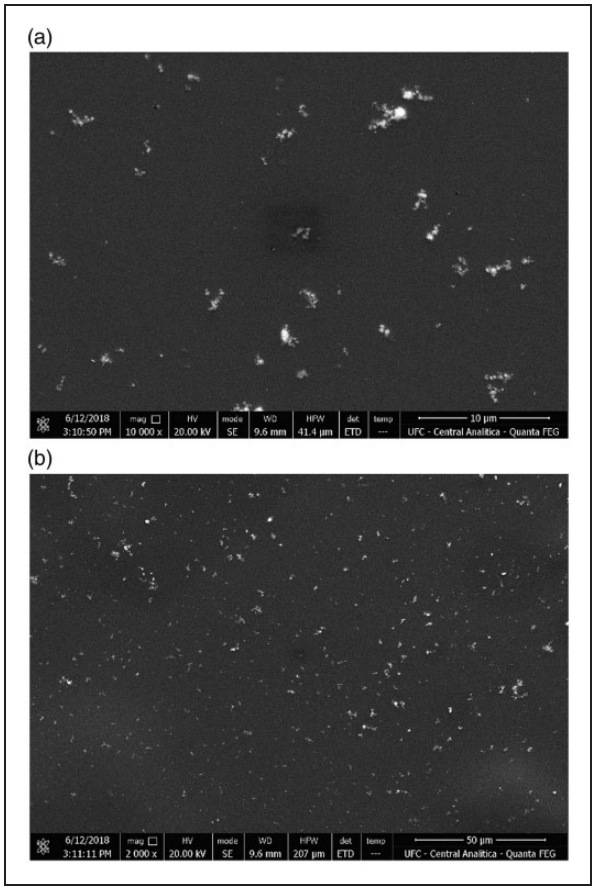

Figure 6. Micrograph of the selective surface sample of CNSL technical, with magnification factor of: (a) 10,000× and (b) 2000×.

equation (9). Subsequently, the values obtained of absorbance were applied in the equation (7) to obtain the values of emissivity. Thus, to compare the efficiencies (f) of all selective surfaces, the absorptivity is divided by the emissivity. For values $f > 18$, the surface is considered highly selective. The data obtained are shown in Table 5.

It is observed that the surface composed of technical CNSL has an absorptivity value and an efficiency superior to that of natural CNSL and commercial surfaces. However, the emissivity values were very near. It is worth noting that on the other days of tests, the values obtained were similar to the values presented in Table 5.

The surface produced has an average thickness of 2000 nm, while the commercial surface (MRTiNOX)

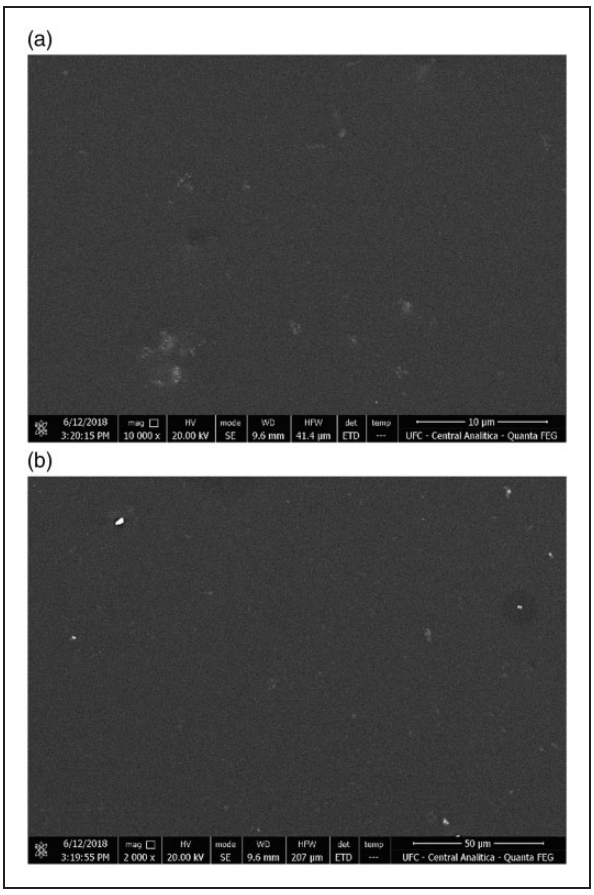

Figure 7. Micrograph of the selective surface sample of CNSL natural, with magnification factor of: (a) 10,000× and (b) 2000×.

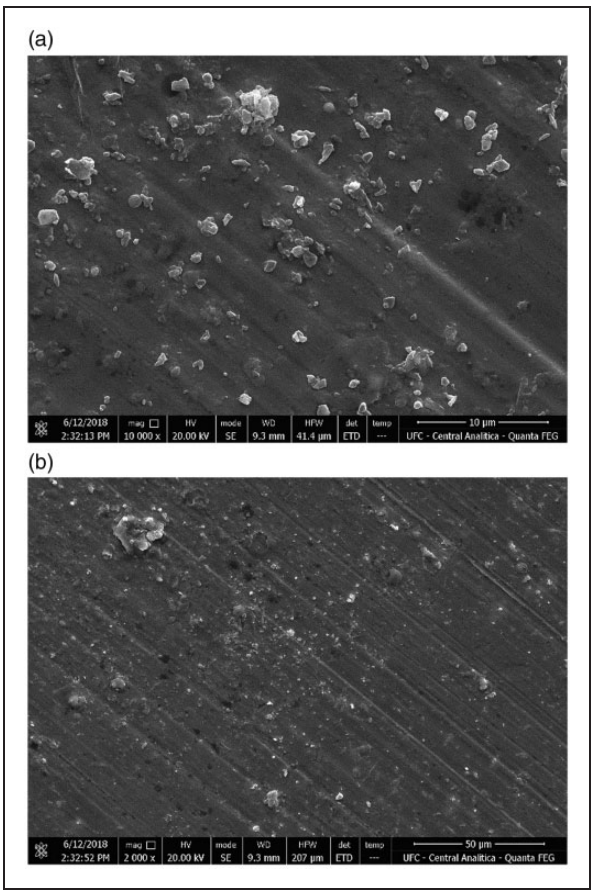

Figure 8. Micrograph of the MRTiNOX selective surface sample, with magnification factor of: (a) 10,000× and (b) 2000×.

has a thickness of 250 nm, so the surface produced is eight times larger than the commercial surface. Therefore, this is a factor that can be optimized to achieve better absorbance values.

Analyzes in the SEM

Figures 7 and 8 show SEM images with increased of 10,000 × and 200 ×, respectively. The micrographs obtained showed the distribution of the selective surface on the copper substrate after the heat treatment, following the composition presented in Table 1.

Figure 6 shows the SEM of the surface containing technical CNSL, in which it is possible to verify exposed grains containing oxygen, copper, and bismuth.

Figure 7 shows the SEM for the surface containing natural CNSL, in which it is possible verify exposed grains containing oxygen, copper, and bismuth. However, as observed in the SEM of the technical CNSL, in the EDX some peak were not identified, but possibly be the peaks of carbon and hydrogen. Both in Figures 7 and 8, it is possible verify a sample with a good deposition, since the grains found in the surfaces are evenly spread.

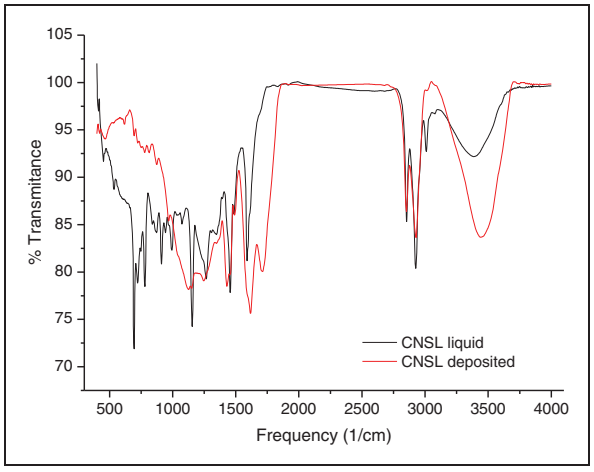

Figure 9. Sample transmittance graph with technical CNSL.

In the commercial surface (MRTiNOX), Figure 8, it is seen that the copper substrate was practically filled. Note also due to the diagonal lines present in the material, a preferred direction in the application of the selective surface. It is observed dispersed grains of the main matrix are visualized, being identified: oxygen, nickel, aluminum, and chromium.

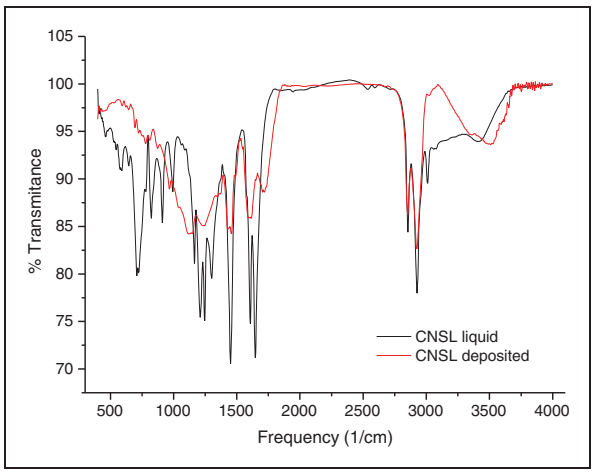

Figure 10. Sample transmittance graph with nature CNSL.

Infrared analysis

With infrared analysis, we can identify the presence of some component after the process of heat treatment in the kiln. Thus, the analysis of the CNSL liquid and the CNSL deposited after heating for the technical and natural CNSL was performed.

Figures 9 and 10 show the infrared analysis for the technical CNSL and the natural CNSL, respectively. Some characteristic peaks are observed in the liquid CNSL and in the deposited CNSL. However, it observes the interference of moisture in the analysis, because in these spectra in KBr pellets, it has contact with the air in the sample preparation, it is observed that the characteristic bands of OH around 3300 are quite intense as also in 1640 that is derived from the angular deformation of the OH of water molecules.

Conclusions

Based on the results obtained, it was verified that the selective surfaces produced obtained results similar to commercial surface MRTiNOX. The selective surface containing technical CNSL presented values closer to the commercial surface, obtaining an equal absorptivity and an efficiency slightly higher than the MRTiNOX. Therefore, it was found that the technician CNSL, mainly, can be an alternative for selective surfaces in solar collectors.

It should be noted that the deposition technique used was satisfactory. However, other deposition techniques can be tested in order to improve the deposition process of the sample in the substrate.

Acknowledgments

The laboratory technique Nadia Aline de Oliveira Pitombeira, for conducting the infrared analysis and the absorbance tests, in the Chemistry Department of the UFC; The Central Analytical of the UFC, by the characterization by MEV; The teachers Paulo Alexandre and Maria Eugênia, from the Laboratory of Solar Energy and Natural Gas, for yielding a space for the tests in the sun, as well as for providing the data of solar radiation in the days of the field tests; The company Cione for having made available the CNSL technical; Funcap for financial support; Capes.

Declaration of conflicting interests

The author(s) declared no potential conflicts of interest with respect to the research, authorship, and/or publication of this article.

Funding

The author(s) received financial support for the research through of the fundação cearense de apoio ao desenvolvimento científico e tecnológico (Funcap).

ORCID iDs

Diego Caitano Pinho https://orcid.org/0000-0001-9324-3375
Paulo Alexandre Costa Rocha https://orcid.org/0000-0002-4366-366X

References

1. Selvakumar N and Barshilia HC. Review of physical vapor deposited (PVD) spectrally selective coatings for mid- and high-temperature solar thermal applications. *Solar Energy Mater Solar Cells* 2012; 98: 1–23.
2. Medeiros IDM, Gomes KC, Gonçalves RPN, et al. Selective solar surface solar based on black chromium: influence of electrodeposition parameters in the absorption of surfaces. *Mater Res* 2019; 22: 1–6.
3. Blaschke T, Biberacher M, Gadocha S, et al. Energy landscapes: meeting energy demands and human aspirations. *Biomass Bioenergy* 2013; 55: 3–16.
4. Kabir E, Kumar P, Kumar S, et al. Solar energy: potential and future prospects. *Renew Sustain Energy Rev* 2017; 82: 894–900.
5. Ramos REB. Análise de desempenho de um fogão solar construído a partir de sucatas de antena de TV. Master's degree, Universidade Federal do Rio Grande do Norte, Natal, 2011.
6. Banthuek S, Suriwong T, Nunocha P, et al. Application of Ni-Al_2O_3 cermet coating on aluminium fin a the solar absorber in evacuated tube collector (ETC). *Mater Today Proc* 2018; 5: 14793–14798.
7. Bassett AW, Breyta CM, Honnig AE, et al. Synthesis and characterization of molecularly hybrid bisphenols derived from lignin and CNSL: application in thermosetting resins. *Eur Polym J* 2019; 111: 95–103.
8. Moreira MM, Silva LRR, Mendes TAD, et al. Synthesis and characterization of a new methacrylate monomer derived from the cashew nut shell liquid (CNSL) and its effect on dentinal tubular occlusion. *ScienceDirect* 2018; 24: 1144–1153.
9. Balachandran VS, Jadhav SR, Vemula PK, et al. Recent advances in cardanol chemistry in a nutshell: from a nut to nanomaterials. *Chem Soc Rev* 2013; 42: 413–832.
10. Guissoni ACP, Silva IG, Geris R, et al. Atividade larvicida de Anacardium occidentale como alternativa ao controle de Aedes aegypti e sua toxicidade em Rattus

norvegicus. *Revista Brasileira de Plantas Medicinais* 2013; 15: 363–367.
11. Costa KP, Viveiros BM, Junior MASS, et al. Chemical transformation in technical cashew nut shell liquid and isolated mixture of cardanols, evaluation of the antioxidant activity and thermal stability of the products for use in pure biodiesel. *Fuel* 2019; 235: 1010–1018.
12. Kalogirou AS. Prediction on flat–plate collector performance parameters using artificial neural networks. *Solar Energy* 2006; 80: 248–259.
13. Almecogroup, http://www.almecogroup.com/uploads/9701Specification_TiNOX_energy_EN_V6_%2020180412.pdf (accessed 15 January 2019).
14. Universidade estadual paulista (UNESP), http://www.dem.feis.unesp.br/intranet/tci_capitulo1.pdf (accessed 20 January 2019).